# NJC

## Accepted Manuscript

ROYAL SOCIETY OF CHEMISTRY

www.rsc.org/njc

**SYNTHESIS AND CHARACTERIZATIONS OF NEW TRIPHENYLAMINO-1,8-NAPHTHALIMIDES FOR ORGANIC LIGHT-EMITTING DIODE APPLICATION**

Rungthiwa Arunchai,[a] Taweesak Sudyoadsuk,[b] Narid Prachumrak,[b] Supawadee Namuangruk,[c] Vinich Promarak,[d] Mongkol Sukwattanasinitt[a] and Paitoon Rashatasakhon,[a]*

*[a] Organic Synthesis Research Unit, Department of Chemistry, Faculty of Science, Chulalongkorn University, Bangkok, 10330, Thailand*

*[b] Department of Chemistry and Center of Excellence for Innovation in Chemistry, Faculty of Science, Ubon Ratchathani University, Ubon Ratchathani, 34190, Thailand*

*[c] Nanoscale Simulation Laboratory, National Nanotechnology Center (NANOTEC), National Science and Technology Development Agency (NSTDA), Klong Luang, Pathumthani, 12120, Thailand*

*[d] School of Chemistry and Center of Excellence for Innovation in Chemistry, Institute of Science, Suranaree University of Technology, Muang District, Nakorn Ratchasima, 30000, Thailand*

*E-mail: paitoon.r@chula.ac.th                    Tel: 02-218-7620

**Abstract**

Three new triphenylamino naphthalimides (**TPN1-3**) are successfully synthesized by means of Suzuki cross-coupling between *N*-phenyl-1,8-naphthalimide and triphenylamine precursors. In $CHCl_3$ solution phase, their maximum absorption wavelengths are around 430-433 nm while the maximum emission wavelength at 564-599 nm with quantum yields in the range of 0.34 to 0.55 in $CHCl_3$. In solid thin-film state where the packing force enhances the conjugated system and prevents the molecular vibration, their absorption bands move towards longer wavelengths and the emission peaks shift to shorter wavelengths. These compounds show excellent thermal stabilities with the 10% weight loss temperatures well above 350 °C. Results from the electrochemical investigation by cyclic voltammetry agrees with the data from computational calculations using Gaussian 09 program with B3LYP/6-31G(d,p) geometry optimizations. When the multi-layer OLED device of structure ITO/PEDOT:PSS/**TPN1**:CBP/BCP/LiF/Al is fabricated, a maximum brightness of 10,404 $cd/m^2$ of yellowish green light at an applied voltage of 19 V with a turn-on voltage of 5.8 V are observed. The effect of solubility of these compounds on device performance is proven by AFM images of the spin-casted thin films.

**Keywords**: Triphenylamine, Naphthalimide, Suzuki cross-coupling, OLED, Emissive material

## 1. Introduction

Organic light-emitting diodes (OLEDs) are considered to be the next generation of flat panel displays after the LCD and plasma technologies due to their key advantages such as low energy consumption, high brightness, light weight, and possibility for fabrication into large and flexible displays [1]. Since the working principle of OLED involves the recombination of

electron and hole in the layer of emissive material, the color of an OLED device thus depends primarily on the electronic properties of this material [2]. Apart from the typical aluminum-hydroxyquinoline complex (Alq$_3$) and some other coordination complexes of transition metals [3], purely organic compounds such as pyrene derivatives [4] and tetraphenylsiloles [5] have been reported as emissive materials. During our research project on design and synthesis of novel OLED materials, we became interested in the combination of 1,8-naphthalimide and triphenylamine motives into the same molecule since both of them have distinctive photophysical properties. 1,8-Naphthalimide derivatives have been generally used as brilliant dyes in synthetic fiber [6] and fluorescent optical brighteners [7]. They have also been used as electron-deficient organic materials for OLEDs with high performance, good light stability, and high fluorescent quantum yield [8]. When 1,8-naphthalimides are substituted by an electron-donating substituent at the 4-position, the fluorescent quantum yields can be increased and the emission peaks can shift to a longer range [9]. On the other hand, triphenylamine and its derivatives such as *N,N*'-di(1-naphthyl)-*N,N*'-diphenyl-(1,1'-biphenyl)-4,4'-diamine (NPB) are well known for their relatively easy oxidations into the radical-cation intermediates and have been frequently used as hole-transporting materials in OLED [10]. In this paper, we report our studies on synthesis and characterization of triphenylamino-*N*-phenyl-1,8-naphthalimides (**TPN1-TPN3**, **Fig. 1**). The thermal and electrochemical analyses, the computational calculation on HOMO-LUMO energy levels, and the fabrication of these materials into OLED devices are reported herein.
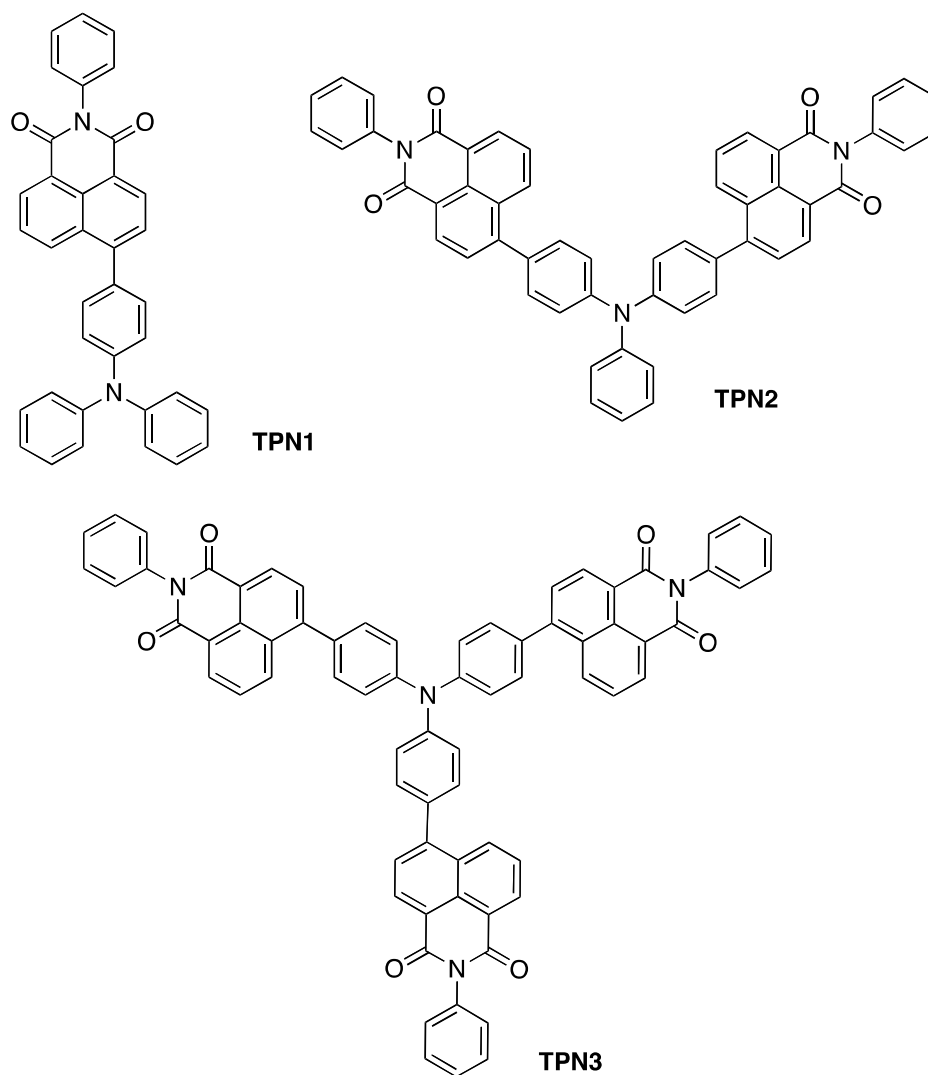
**Fig.1** Structure of target compounds (**TPN1-TPN3**).

## 2. Experimental

### 2.1 Chemical and instruments

All reagents including Pd catalyst, 4-(*N*,*N*-diphenylamino)-phenylboronic acid, and *bis*(pinacolato)diboron were purchased from Aldrich (USA). 4-Bromo-*N*-(phenyl)-1,8-naphthalimide [11], 4,4'-(dibromo)triphenylamine [12], 4,4',4''-(triiodo)triphenylamine [13], and *N*-phenyl-1,8-naphthalimide-4-boronic acid pinacol ester (**A**) [14] were prepared according to the reference procedures. Thin layer chromatography (TLC) was performed on aluminium sheets precoated with silica gel (Merck Kiesegel 60 F$_{254}$) (Merck KgaA,

Darmstadt, Germany). Column chromatography was performed on silica gel (Merck Kieselgel 60G) (Merck KGaA, Darmstadt, Germany). All ^{1}H-NMR spectra were determined on Varian Mercury NMR spectrophotometer (Varian, USA) at 400 MHz with chemical shifts reported as ppm in CDCl$_3$. The ^{13}C-NMR spectra were measured on Bruker Mercury NMR spectrophotometer (Bruker, Germany) which equipped at 100 MHz with chemical shifts reported as ppm in CDCl$_3$. Mass spectra were recorded on a MicrOTOF high resolution mass spectrometer (Bruker Daltonics). Absorption spectra were measured by a Shimadzu UV-2550 UV-Vis spectrophotometer. Fluorescence spectra were obtained from an Agilent technologies Cary Eclipse spectrofluorometer. Fluorescent lifetimes were measured by a Horiba Jobin Yvon FluoroMax 4 (Horiba Jobin Yvon, France) using the time correlated single photon counting method with the following settings: excitation source, 370 nm NanoLED; time range, 100 ns; peak preset 10,000 counts; repetition rate at 1 MHz; coaxial delay of 60 ns. The FT-IR spectra were recorded between 400 cm$^{-1}$ to 4,000 cm$^{-1}$ in transmittance mode on a Fourier Transform Infrared Spectrophotometer Impact 410 (Nicolet Instruments Technologies, Inc, WI, USA). Cyclic voltammograms were obtained from an Autolab voltammetry instrument. Elemental (CHN) analyses were performed on Perkin-Elmer 2400 series II (Perkin-Elmer, USA).

## 2.2 Synthesis

### 2.2.1   TPN1

Under a N$_2$ atmosphere, a mixture of 4-(*N*,*N*-diphenylamino)-phenylboronic acid (0.10 g, 0.36 mmol), 4-bromo-*N*-(phenyl)-1,8-naphthalimide (0.14 g, 0.41 mmol), and Pd(dppf)Cl$_2$ (22 mg, 0.03 mmol) in toluene (10 mL) was stirred. Then an aqueous solution of K$_2$CO$_3$ (2 M 1 mL) was added via syringe. The reaction mixture was heated at 60 °C for 72 h. After cooling to room temperature, the reaction was diluted with water and extracted with CH$_2$Cl$_2$. The combined organic phase was dried over anhydrous MgSO$_4$, filtered, and concentrated

under reduced pressure. The crude product was purified by column chromatography using CH$_2$Cl$_2$ as the eluent to afford **TPN1** as yellow solid (0.15 g, 84%). IR (ATR, cm$^{-1}$): ν 3059, 1655, 1585, 1488, 1368, 1231. $^1$H-NMR (400 MHz, CDCl$_3$, ppm) δ 8.71 – 8.65 (m, 2H), 8.48 (dd, $J$ = 8.5 and 1.0 Hz, 1H), 7.76 (t, $J$ = 7.9 Hz, 2H), 7.58 (dd, $J$ = 10.3 and 4.7 Hz, 2H), 7.52 – 7.46 (m, 1H), 7.44 – 7.38 (m, 2H), 7.38 – 7.29 (m, 6H), 7.24 (ddd, $J$ = 7.5, 5.2, and 2.5 Hz, 6H), 7.11 (t, $J$ = 7.3 Hz, 2H). $^{13}$C-NMR (100 MHz, CDCl$_3$, ppm) δ 164.5, 164.3, 148.5, 147.4, 147.2, 135.6, 133.2, 131.9, 131.6, 131.3, 130.8, 130.2, 129.5, 129.4, 129.3, 128.70, 128.65, 127.8, 126.8, 125.1, 123.7, 123.1, 122.5, 121.4. Anal. Calcd. for C$_{36}$H$_{24}$N$_2$O$_2$: C, 83.70; H, 4.68; N, 5.42. Found: C, 83.83; H, 4.59; N, 5.32. HRMS: *m/z* calcd for C$_{36}$H$_{24}$N$_2$O$_2$: 516.1838; found: 539.1736 [M+Na]$^+$

### 2.2.2   TPN2

This compound was prepared from 4,4'-(dibromo)triphenylamine (1 eq) and boronate ester **A** (2.6 eq) using the same conditions for the synthesis of **TPN1**. The crude product was purified by column chromatography using pure CH$_2$Cl$_2$ as the eluent to afford as yellow solid in 30% yield. IR (ATR, cm$^{-1}$): ν 3059, 1655, 1585, 1488, 1368, 1231. $^1$H-NMR (400 MHz, CDCl$_3$, ppm) δ 8.70 (d, $J$ = 7.5 Hz, 4H), 8.48 (t, $J$ = 7.4 Hz, 2H), 7.79 (dt, $J$ = 8.3 and 4.1 Hz, 4H), 7.58 (t, $J$ = 7.4 Hz, 4H), 7.50 (dd, $J$ = 8.0 and 3.7 Hz, 6H), 7.44 (d, $J$ = 8.4 Hz, 1H), 7.37 (dt, $J$ = 8.4 and 5.5 Hz, 10H), 7.21 (dd, $J$ = 8.0 and 6.5 Hz, 2H). $^{13}$C-NMR (100 MHz, CDCl$_3$, ppm) δ 164.5, 164.3, 147.9, 146.9, 135.5, 133.1, 133.0, 131.7, 131.3, 131.2, 131.1, 130.2, 129.8, 129.4, 129.3, 128.8, 128.7, 127.9, 126.9, 125.8, 124.5, 123.9, 123.6, 123.1, 121.6. Anal. Calcd. for C$_{54}$H$_{33}$N$_3$O$_4$: C, 82.32; H, 4.22; N, 5.33. Found: C, 83.55; H, 4.39; N, 5.12. HRMS: *m/z* calcd for C$_{54}$H$_{33}$N$_3$O$_4$: 787.2471; found: 810.2368 [M+Na]$^+$.

### 2.2.3   TPN3

This compound was prepared from 4,4',4''-(triiodo)triphenylamine (1 eq) and boronate ester **A** (9.0 eq) using the same conditions for the synthesis of **TPN1**. The crude product was purified by column chromatography using pure $CH_2Cl_2$ to $CH_2Cl_2$/EtOAc (20/1) as the eluent to afford as orange solid in 56% yield. IR (ATR, cm$^{-1}$): ν 3059, 1655, 1585, 1488, 1368, 1231. $^1$H-NMR (400 MHz, CDCl$_3$, ppm) δ 8.71 (d, 6H), 8.51 (d, $J$ = 7.7 Hz, 3H), 7.82 (d, $J$ = 7.3 Hz, 6H), 7.50 (m, br, 21H), 7.35 (d, $J$ = 7.2 Hz, 6H). $^{13}$C-NMR (100 MHz, CDCl$_3$, ppm) δ 164.4, 164.2, 147.6, 146.6, 135.4, 133.9, 132.9, 131.7, 131.3, 131.2, 130.2, 129.4, 129.3, 128.74, 128.66, 127.9, 126.9, 124.5, 123.2, 122.4, 121.8. Anal. Calcd. for $C_{72}H_{42}N_4O_6$: C, 81.65; H, 4.00; N, 5.29. Found: C, 81.90; H, 4.14; N, 5.11. HRMS: *m/z* calcd for $C_{72}H_{42}N_4O_6$: 1058.3104; found: 1081.3005 $[M+Na]^+$.

### 2.3 Electrochemical analysis

In the CV experiments, platinum wire was used as a counter electrode, Ag/AgNO$_3$ as a reference electrode and platinum as a working electrode. Ferrocene was used as an external standard. *Tetra*-n-butylammonium hexafluorophosphate (TBAPF$_6$) was used as an electrolyte in 20% MeCN in $CH_2Cl_2$. The concentration of electrolyte was 0.1 M, and the concentration of **TPN1**, **TPN2** and **TPN3** was 1.0 mM and a scan rate was 50 mV/s. The HOMO energy levels were calculated from the onset of oxidation potential (E$_{onset}$) according to a formula, HOMO = -(E$_{onset}$ – E$_{Fc/Fc+}$ + 4.8). The LUMO energy levels were calculated by subtracting the HOMO energy levels with the band gaps energy estimated from the onset of UV–Vis absorption.

### 2.4 Quantum chemical calculation method

The ground state geometries of the compounds were optimized by density functional theory (DFT) at B3LYP/6-31G(d,p) method in gas phase without any constraint. The highest occupied molecular orbital (HOMO), lowest occupied molecular orbital (LUMO), and energy

difference between HOMO and LUMO ($\Delta_{H-L}$) were analyzed at the ground state. The lowest

vertical excitation energy ($E_{ex}$) from ground to excited state was calculated by time-

dependent DFT at TD-B3LYP/6-31G(d,p) level of theory. All calculations were performed

by Gaussian 09 program package [15].

## 3.  Results and Discussion

### 3.1 Synthesis of **TPN1-TPN3**

The synthesis of our target compounds relies on the Suzuki cross-coupling reactions (**Scheme 1**). Such reaction between the readily accessible 4-bromo-*N*-(phenyl)-1,8-naphthalimide and the commercially available 4-(*N,N*-diphenylamino)-phenylboronic acid under the catalysis of (dppf)PdCl$_2$ provided **TPN1** in excellent yield of 84%. The conversion of 4-bromo-*N*-(phenyl)-1,8-naphthalimide into the pinacol boronate ester **A** was carried out using the procedure reported in the literature [14]. The Suzuki reaction between **A** and 4,4'-(dibromo)triphenylamine or 4,4',4''-(triiodo)triphenylamine afforded **TPN2** or **TPN3** in moderate yields. The characterization by IR, NMR, and HR-MS confirmed the successful synthesis of these target compounds.
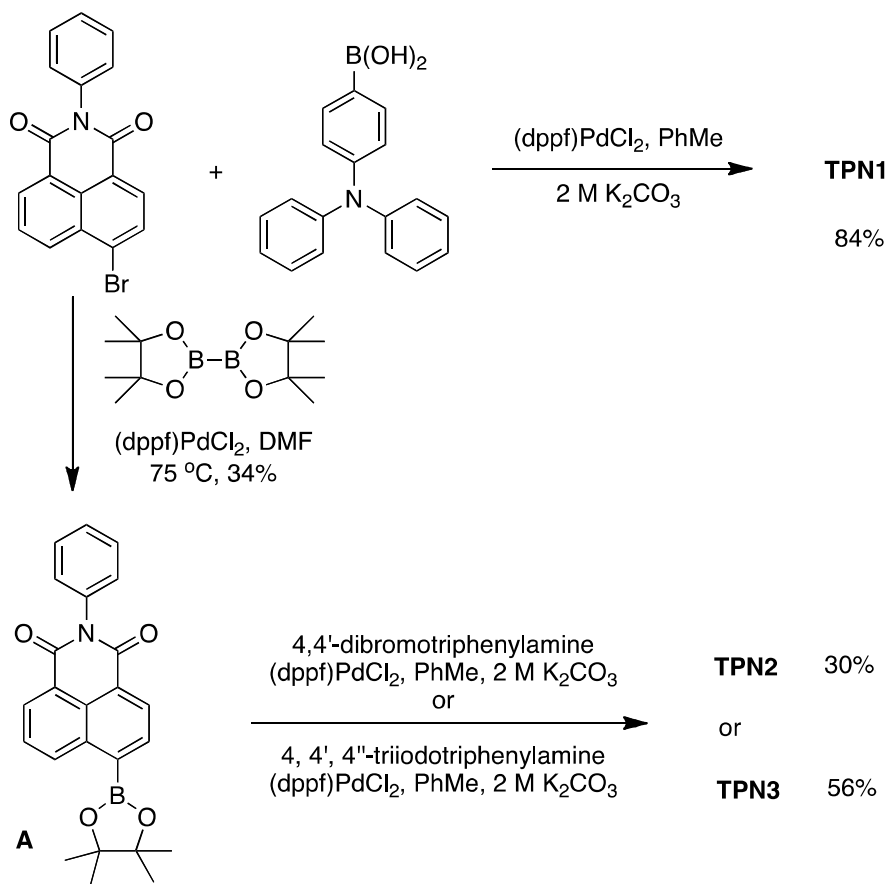
**Scheme 1** Synthesis of **TPN1-3**

*3.2 Photophysical properties*

The absorption and emission properties of **TPN1-3** in both CHCl$_3$ solution and spin-casted thin film were investigated and summarized in **Table 1**. In solution phase, each compound exhibited a characteristic π-π* transition as observed by the absorption peak around 312-326 nm, along with a charge transfer between the naphthalimide(s) and triphenylamine group evidenced by the absorption peak around 430-433 nm (**Fig. 2**). Therefore, the molar extinction coefficient of the latter peak increases with the numbers of naphthalimide unit. In the solid state, the absorption spectra of these compounds also have the same pattern as in solution phase (**Fig.3**). However, the maximum absorption wavelengths appear at longer ranges (316-336 and 435-437 nm) due to more efficient π-conjugation between the

naphthalimide and triphenylamine groups in the solid state, which may cause by the restricted molecular vibration and rotation.

**Table 1** Photophysical properties of **TPN1-3** in CHCl$_3$ solutions and spin-casted thin films.

| Cmpd. | CHCl$_3$ solution | | | | | | | Thin film | |
|---|---|---|---|---|---|---|---|---|---|
| | $\lambda_{max}{}^{Abs}$ (nm) | Log ε (M$^{-1}$cm$^{-1}$) | $\lambda_{max}{}^{Emis}$ (nm) [a] | $\Phi$ [b] | $\tau_{ave}$ (ns) [c] | $k_r$ (ns$^{-1}$) [d] | $k_{nr}$ (ns$^{-1}$) [e] | $\lambda_{max}{}^{Abs}$ (nm) | $\lambda_{max}{}^{Emis}$ (nm) |
| **TPN1** | 312 | 4.37 | 599 | 0.34 | 7.14 | 0.0476 | 0.0924 | 316 | 555 |
| | 433 | 4.03 | | | | | | 435 | |
| **TPN2** | 322 | 4.57 | 580 | 0.49 | 6.58 | 0.0745 | 0.0775 | 326 | 551 |
| | 431 | 4.36 | | | | | | 435 | |
| **TPN3** | 326 | 4.65 | 564 | 0.55 | 6.11 | 0.0900 | 0.0736 | 336 | 550 |
| | 430 | 4.51 | | | | | | 437 | |

[a] Excited at the shorter maximum absorption wavelength. [b] Quantum yield determined in CHCl$_3$ solution (A<0.1) at room temperature with the excitation wavelength at the longer absorption maxima of each compound. Fluorescein in 0.1 M NaOH(aq) ($\Phi_F = 0.91$) was used as the standard. [c] Average fluorescent decay times. [d] Radiative rate estimated from $\Phi/\tau_{ave}$. [e] Non-radiative rate estimated from $(1-\Phi)/\tau_{ave}$.
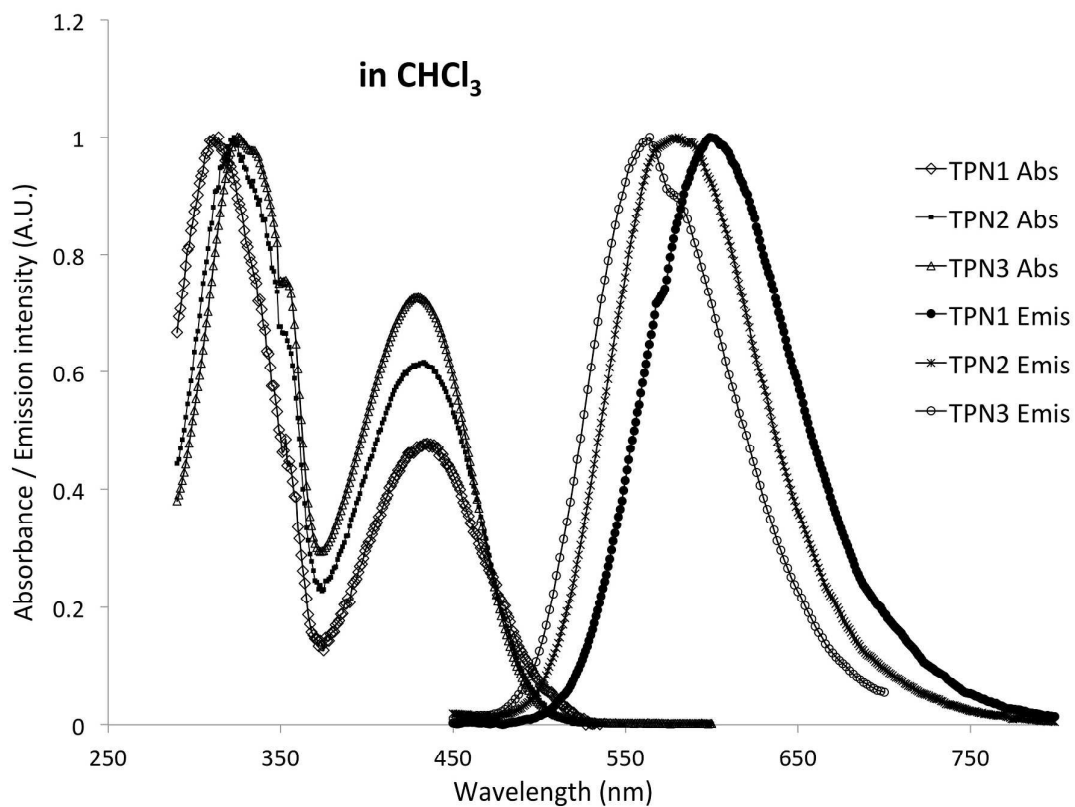
**Fig. 2** Normalized absorption and emission spectra of **TPN 1-3** in CHCl$_3$ (15 μM). The excitation wavelengths were at 430 nm.
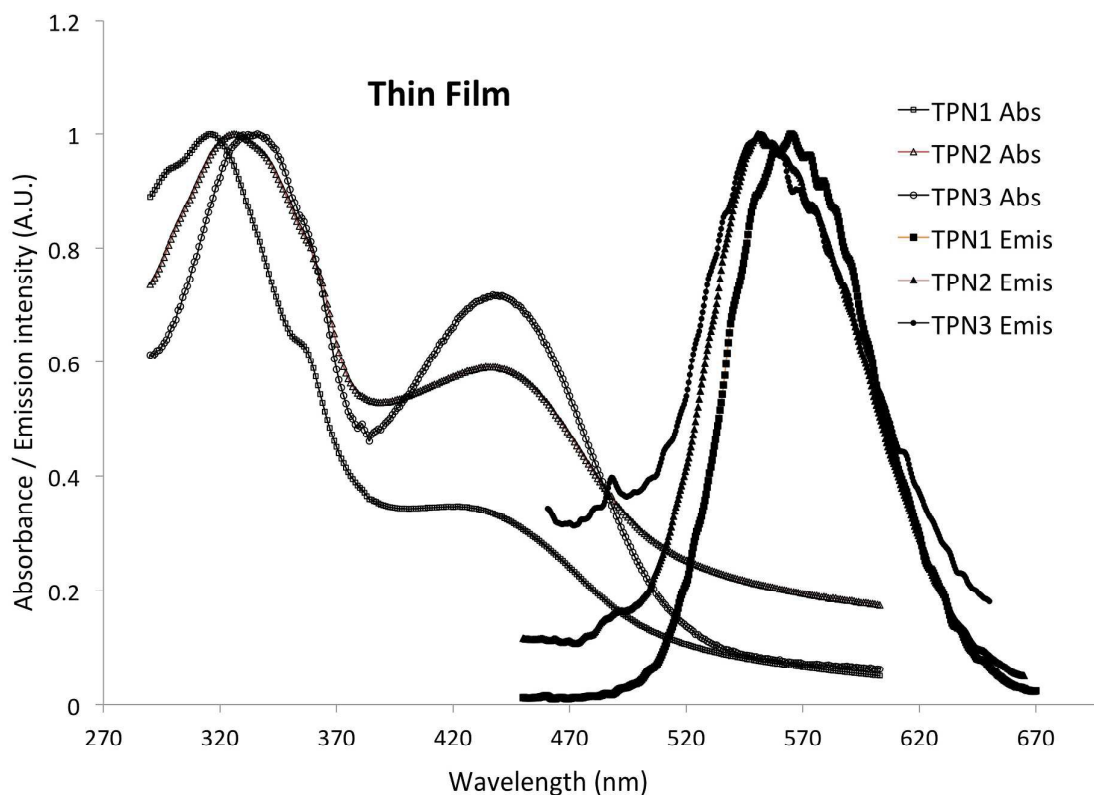
**Fig. 3** Normalized absorption and emission spectra of spin-casted film of **TPN 1-3**. The excitation wavelengths were at 435 nm.

The normalized fluorescence spectra in solution phase are also shown in **Fig. 2**. **TPN1**, **TPN2**, and **TPN3** exhibited a maximum emission wavelength at 599, 580, and 564 nm, respectively. With the increase in the number of naphthalimide groups, the fluorescence emission peaks are gradually blue-shifted due to a decrease in electron delocalization between the donor and the acceptor. The quantum yields of these compounds increase with the number of naphthalimide units as **TPN3** has the highest quantum yield of 0.55. The data from average fluorescent decay time also suggested that excited **TPN3** possesses the fastest radiative rate ($k_r$) and the slowest non-radiative rates ($k_{nr}$). As for the emission spectra of thin-film, the packing force and the restricted structural rotation in the solid state shifted all of the photoluminescent spectra towards shorter wavelengths at 550-555 nm (**Fig. 3**).

*3.3 Thermal properties*

The thermal properties of all compounds were determined by thermogravimetric analysis (TGA) and differential scanning calorimetry (DSC) with a heating rate of 10 °C/min under nitrogen atmosphere. The TGA curves (**Fig. 4a**) revealed that all **TPN1**, **TPN2**, and **TPN3** were thermally stable with high 10% weight loss temperatures ($T_d^{10}$) at 398, 453 and 527°C, respectively. This trend in thermal stabilities might be attributed to the increasing molecular weight. Since the morphological changes might be promoted by rapid molecular motion at higher temperature, amorphous materials with high glass transition temperature ($T_g$) are usually preferred for OLED materials. From the DSC experiment on **TPN1** (**Fig. 4b**), one sharp endothermic peak at 264 °C due to melting temperature ($T_m$) and no glass transition temperature suggested that **TPN1** is a crystalline material. For both **TPN2** and **TPN3**, there were endothermic baseline shifts which indicated glass transition temperature at 254 °C. The melting temperature of **TPN2** and **TPN3** were at 385 and 477 °C, respectively. These abilities to form molecular glasses with high thermal stabilities are highly desirable for optoelectronic materials casted into thin films by vacuum evaporation or solution casting processes.

13
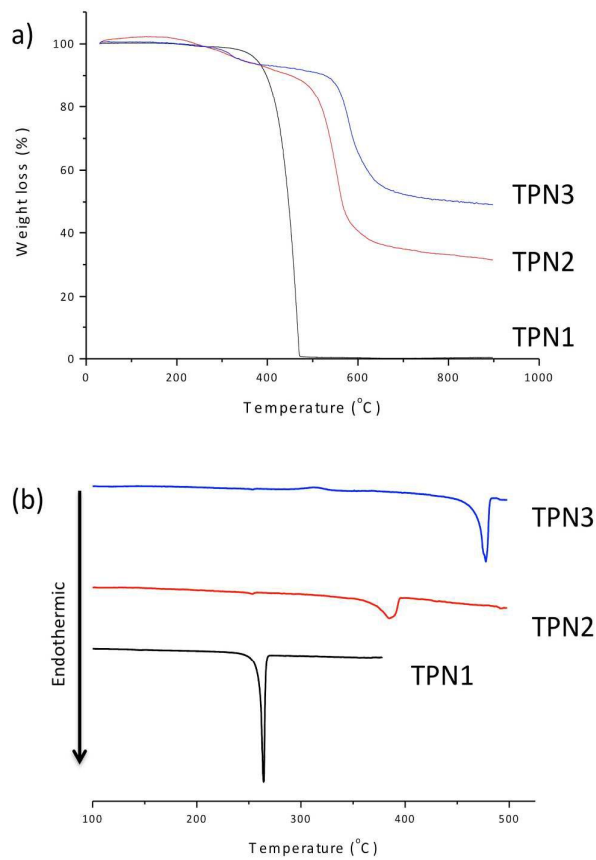
**Fig.4** a) TGA thermograms and b) second DSC traces of **TPN1**, **TPN2** and **TPN3**

**Table 2** Thermal properties of **TPN1-3.**

| Compounds | $T_g^a$ ($^oC$) | $T_m^a$ ($^oC$) | $T_d^b$($^oC$) |
|-----------|-----------------|-----------------|----------------|
| **TPN1**  | -               | 264             | 398            |
| **TPN2**  | 254             | 385             | 453            |
| **TPN3**  | 254             | 477             | 527            |

[a] Obtained from DSC measurements on the second heating cycle with a heating rate of 10 $^oC$/min under $N_2$. [b]10% weight loss temperature obtained from TGA measurement with a heat rate of 10 $^oC$/min under $N_2$.

14

*3.4 Electrochemical analysis*

**Table 3** The experimental and calculated electrochemical properties of **TPN1-3**.

| Cmpd. | Experimental data | | | | Calculated data[e] | | | | |
|---|---|---|---|---|---|---|---|---|---|
| | $E_g$ | $E_{onset}$ | HOMO | LUMO | $\lambda_{ex}$ | $E_{ex}$ | $\Delta_{H-L}$ | HOMO | LUMO |
| | $(eV)^a$ | $(V)^b$ | $(eV)^c$ | $(eV)^d$ | $(nm)^f$ | $(eV)^f$ | $(eV)^g$ | (eV) | (eV) |
| **TPN1** | 2.48 | 0.51 | -5.21 | -2.73 | 487 | 2.54 | 2.92 | -5.22 | -2.30 |
| **TPN2** | 2.52 | 0.53 | -5.23 | -2.71 | 481 | 2.58 | 2.97 | -5.42 | -2.45 |
| **TPN3** | 2.54 | 0.55 | -5.25 | -2.71 | 467 | 2.65 | 3.04 | -5.58 | -2.53 |

[a] The optical energy gap estimated from the onset of the absorption spectra ($E_g = 1240/\lambda_{onset}$). [b] Onset oxidation potential estimated from the cyclic voltammogram. [c] Estimated by the empirical equation: HOMO = -($E_{onset}$ – $E_{Fc/Fc+}$ + 4.8). [d] Estimated from LUMO = HOMO + $E_g$. [e] Geometry optimizations were done by B3LYP/6-31G(d,p) method. [f] Lowest excitation energy (the first absorption peak) were calculated by TD-B3LYP/6-31G(d,p) method (no solvent is included). [g] $\Delta_{H-L}$ is the energy difference between HOMO and LUMO calculated by TD-B3LYP/6-31G(d,p) method.

The experimental and computationally calculated electrochemical properties are summarized in **Table 3**. The cyclic voltammograms acquired by the anodic scans at room temperature exhibit one reversible oxidation peak for each compound, which might be attributed to the electron-donating ability of triphenylamine moiety. The HOMO energy levels were obtained from the onset oxidation potential ($E_{onset}$) observed on the cyclic voltammograms, and the LUMO energy levels were estimated from the $E_g$ and HOMO data. The $E_{onset}$ were influenced and shifted toward more positive potentials with the increase of naphthalimide units. This data indicated the stabilization of the HOMO level due to the electron-withdrawing

characteristic of naphthalimide group. It is noted that when the number of naphthalimides is increased, the measured HOMO is stabilized from -5.21 eV, -5.23 eV, and -5.25 eV while the LUMO is increased from -2.73 eV, -2.71, and -2.71 eV for **TPN1**, **TPN2**, and **TPN3**, respectively. These cause the wider band gap which increases as the order; 2.48 eV (**TPN1**) < 2.52 eV (**TPN2**) < 2.54 eV (**TPN3**). The tendencies of the experimental Eg, HOMO, and LUMO are well consistent with the calculated values as shown in Table 3. In calculations, both $\Delta_{H-L}$ and $E_{ex}$ are widely used to qualitatively determine the experimental $E_g$ in relatively order. As shown, the $E_{ex}$ is more relatively accurate than the $\Delta_{H-L}$ since it is calculated by the TD-DFT which provided the excitation directly. The orbital plots show exclusive electron localizations at the triphenylamine pendant for the HOMOs, and at the napthalimide fragments for the LUMOs (**Fig. 5**). Since these HOMO and LUMO levels are larger than the work functions of ITO and LiF/Al (**Fig. 6**), these materials can be fabricated into OLED devices using these electrodes. In addition, there is also a possibility of using the commercially available PEDOT:PSS as the hole-transporting layer and BCP as the hole-blocker.
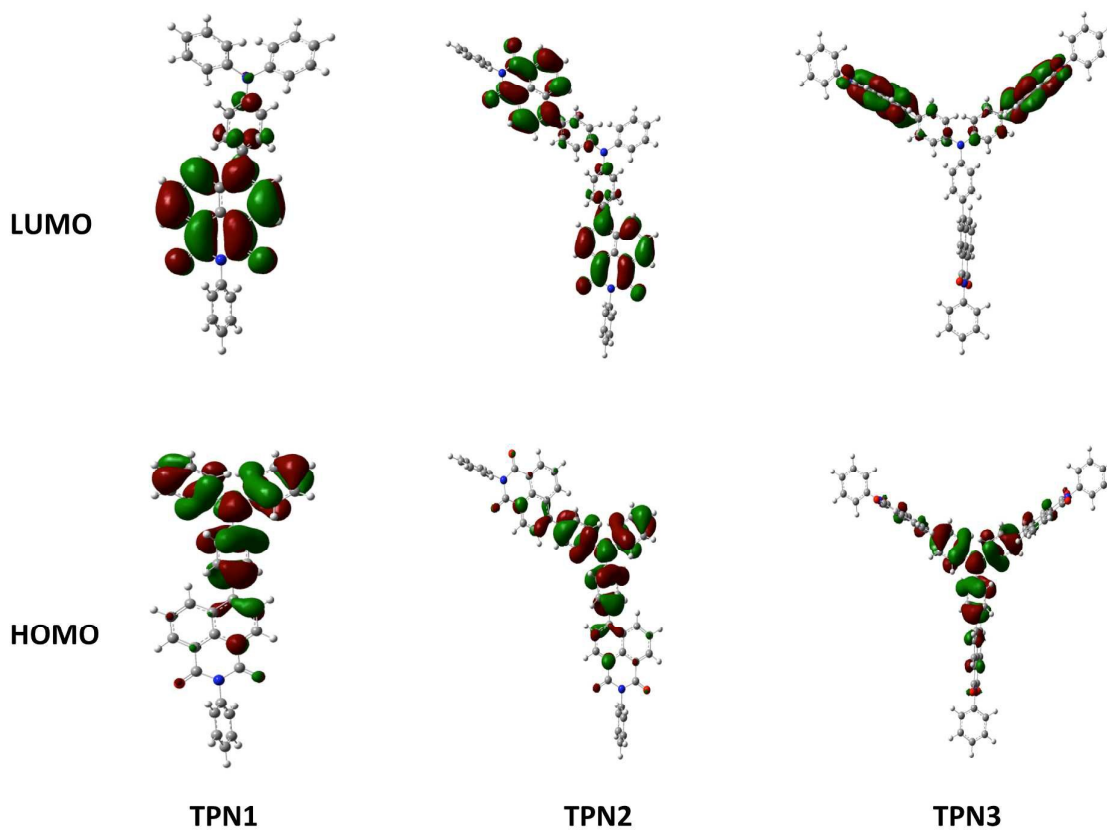
**Fig. 5** Frontier orbital plots for **TPN1-3**.
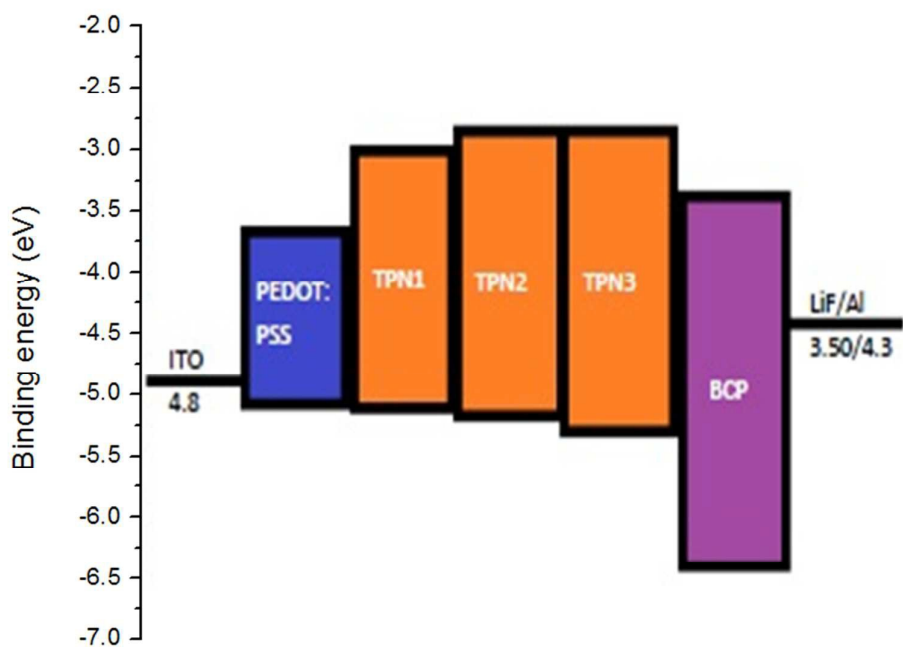


**Fig. 6** Band diagrams of ITO, PEDOT:PSS, **TPN1, TPN2, TPN3**, BCP and LiF/Al.

*3.5 OLED device fabrication*

For the preliminary investigation on material performances and their electroluminescence, five non-optimized OLED devices were fabricated between the ITO and LiF/Al electrodes using PEDOT-PSS as the hole-injection layer (**Fig. 7**). The attempt to fabricate single-layer device using **TPN3** as emissive layer led to poor device performances (Device 1, Table 4), which might results from an improper barrier for electron migration at the interface between emissive layer and the LiF/Al electrode and a poor film-forming ability of **TPN3** due to its low solubility. When a layer of hole-blocking material, dimethyl-4,7-diphenyl-1,10-phenanthroline (BCP), was incorporated (Device 2), slightly improved device performances such as higher maximum luminance were achieved. These devices showed a yellow-orange luminescence with featureless patterns, emission peaks around 586 nm (**Fig. 8**). The EL spectra were red-shifted (~36 nm) from the thin-film PL spectrum with large full width at half maxima (FWHM) of 151 nm, indicating that the EL originates from the emission of the excimer species. This is due to the flat molecular structure of **TPN3**.

We thus fabricated multilayer Device 3-5 using **TPN3-1**-doped 4,4'-bis(*N*-carbazolyl)-1,1'-biphenyl (CBP) as the emissive layer (EML). Under the applied voltages, all fabricated OLEDs (Devices 3-5) emit a bright yellowish green emission with featureless patterns, emission peaks around 530-533 nm, and small FWHM of 75-95 nm (**Fig. 8** and Table 4). The EL spectra of devices 3−5 were identical to their thin-film PL spectra, indicating that the EL purely originates from their corresponding EML. No emission from the host BCP suggesting an efficient energy transfer from the host BCP to **TPN3-1**. Furthermore, no emission shoulder at a longer wavelength resulting from the excimer and exciplex species formed at the interface of the EML and BCP layers is detected. Moreover, stable emission is obtained from all devices, and the EL spectra did not change over the entire driven voltages. Among these diodes, Device 5, which has 6% **TPN1**-doped 4,4'-bis(*N*-carbazolyl)-1,1'-

biphenyl (CBP) as the emissive layer, offers the best performance with a maximum luminance of 10,404 cd/m$^2$ at 19 V, a turn-on voltage of 5.8 V, device luminance efficiency ($\eta_{max}$) of 3.77 cd/A and EQE of 1.11% (**Fig. 9**). This device also showed a current density of 410 mA/m$^2$ and emitted a yellowish green light with the CIE coordinates at (0.295, 0.600). Device 4 using 6% **TPN2**-doped CBP as the EML showed a slightly lower device performance with device luminance efficiency ($\eta_{max}$) of 2.49 cd/A and EQE of 0.73%, while device 3 using 6% **TPN3**-doped CBP as the EML exhibited a poor device performance. Because the electrochemical properties of **TPN1-3** are relatively similar, it was postulated that the efficiency differences in Device 3 to Device 5 might be related to the solubility of these compounds the solvents used in the spin-casting process - CHCl$_3$ and toluene (4:1 v/v). The AFM analysis of casted films revealed that the **TPN1**-doped CBP could form a homogeneous thin film (**Fig. 10**), whereas the **TPN3**-doped CBP film consisted of particles from 0.45 μm or larger. The aggregation of **TPN3** may prohibit the exciton migration, and resulted in the poor device performance.

**Device 1**

**Device 2**

**Device 3**
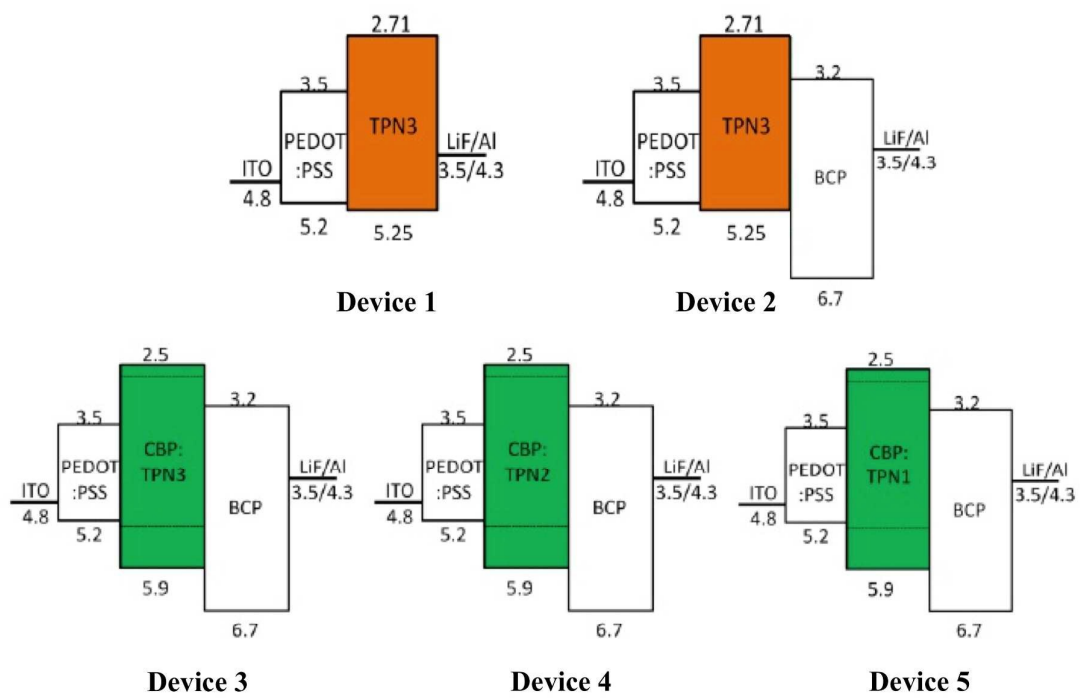
**Device 4**

**Device 5**

**Fig. 7** Structures of Device 1-5
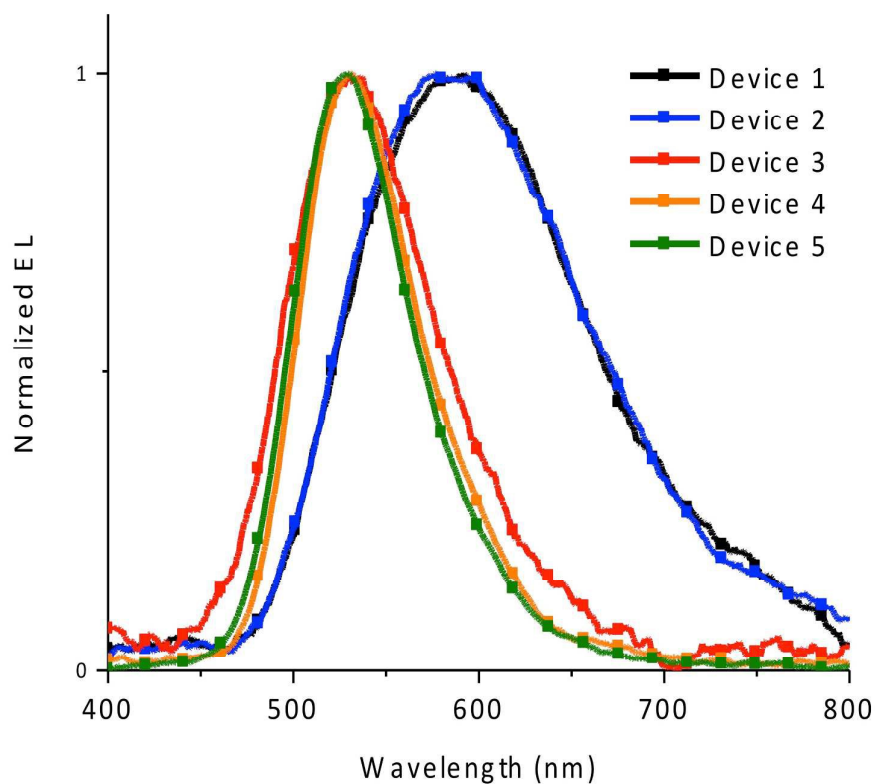
**Fig. 8** Plots of a) EL spectra of the OLEDs (devices 1-5).
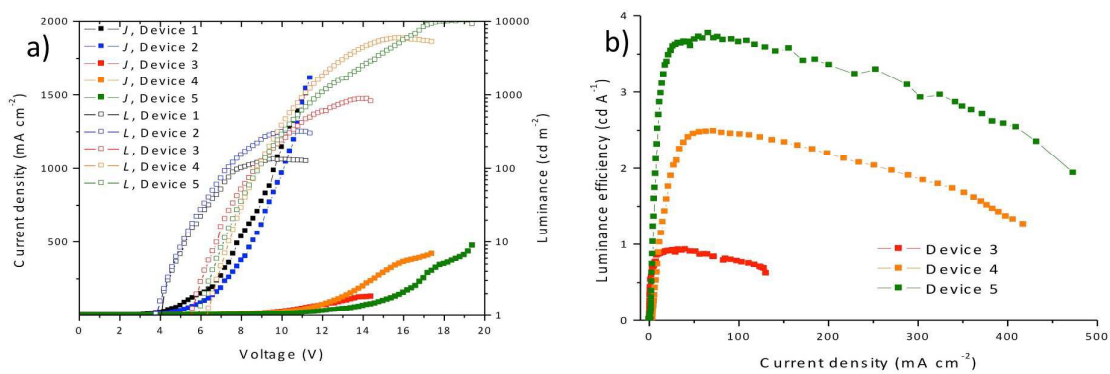


**Fig. 9** a) Current density-luminance-voltage (J-V-L) and b) Efficiency-current density (η-I)

characteristics of the OLEDs (devices 1-5).

**Table 4** Electroluminescent properties of Devices 1-5.

| Device | $\lambda_{EL}$ /FWHM (nm) | $V_{on}$[a] | $L_{max}$ (V)[b] | $\eta_{lum}$[c] | J[d] | $EQE_{max}$[e] | PE[f] | CIE[g] |
|---|---|---|---|---|---|---|---|---|
| 1 | 586/151 | 4.0 | 133 (9.6) | 0.02/7.6V | 985 | 0.006/7.6V | 0.009/6.6V | 0.484, 0.477 |
| 2 | 586/151 | 3.8 | 323 (10.4) | 0.04/8.2V | 1446 | 0.01/8.2V | 0.02/1.0V | 0.487, 0.486 |
| 3 | 533/95 | 5.5 | 877 (14.2) | 0.93/10.8V | 128 | 0.27/10.8V | 0.32/8.4V | 0.258, 0.575 |
| 4 | 531/76 | 6.2 | 5898 (15.8) | 2.49/12.0V | 352 | 0.73/12.0V | 0.68/11.2V | 0.319, 0.604 |
| 5 | 530/75 | 5.8 | 10404 (19.0) | 3.77/14.0V | 410 | 1.11/14.0V | 0.96/11.4V | 0.295, 0.600 |

[a] Turn-on voltage (V). [b] Maximum luminance (cd/m$^2$) (at applied potential V). [c] Luminance efficiency (cd/A). [d] Current density (mA/m$^2$). [e]

Maximum external quantum efficiency (% at V). [f] Power efficiency (lm/W at V). [g] Commission International d'Eclairage coordinates (*x, y*).

TPN1 doped CBP                TPN2 doped CBP                TPN3 doped CBP
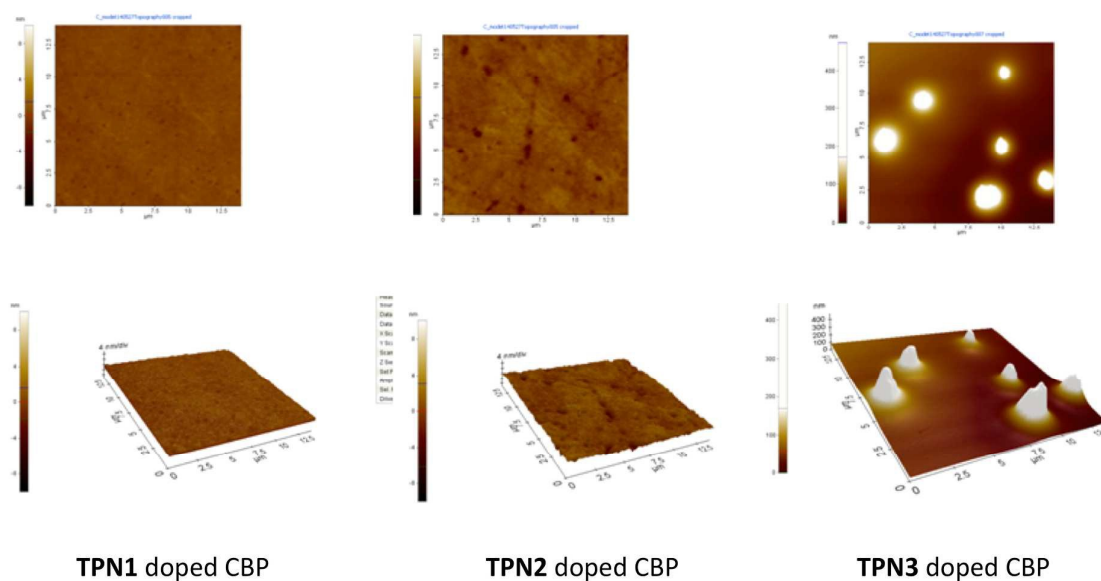
**Fig. 10** AFM images of thin films of CBP doped with **TPN1**, **TPN2**, and **TPN3**

## 4. Conclusion

Three new triphenylamine derivatives substituted by different numbers of *N*-phenylnaphthalimide units were successfully synthesized by means of Suzuki coupling in good to moderate yields. These compounds exhibited absorption maxima around 430 nm and emission maxima around 564-599 nm in CHCl$_3$ solution. The Stoke's shifts were narrower for the spectra of these compounds in solid state as a result of solid packing. With the 10% weight loss temperatures above 350 °C and glass-transition temperature at 254 °C, these compounds showed excellent thermal stability suitable for application as OLED materials. The electrochemical properties were examined by cyclic voltammetry and the data were in good agreement with those obtained from the computational calculations using Gaussian 09 program. The experimental HOMO level of the three compounds were around 5.2 eV while the LUMO levels were around 2.7 eV. When **TPN1**-doped BCP was used as a hole-

transporting material in the OLED device of structure ITO/PEDOT:PSS/**TPN1**:CBP/BCP/LiF/Al, the yellowish green light with a maximum brightness of 10,404 cd/m$^2$ of at an applied voltage of 19 V were observed.

## Acknowledgements

## Reference

[1] L. Xiao, Z. Chen, B. Qu, J. Luo, S. Kong, Q. Gong and J. Kido, *Adv. Mater.,* 2011, **23**, 926.

[2] (*a*) C. W. Tang and S. A. van Slyke, *Appl. Phys. Lett.,* 1987, **51**, 913; (*b*) S. A. Van Slyke, C. H. Chen and C. W. Tang, *Appl. Phys. Lett.,* 1996, **69**, 2160.

[3] D. Kourkoulos, C. Karakus, D. Hertel, R. Alle, S. Schmeding, J. Hummel, N. Risch, E. Holder and K. Meerholz, *Dalton Trans.*, 2013, **42**, 13612.

[4] (*a*) K. R. J. Thomas, N. Kapoor, M. N. K. Prasad Bolisetty, J.-H. Jou, Y.-L. Chen and Y.C. Jou, *J. Org. Chem.*, 2012, **77**, 3921; (*b*) T. S. Kale, K. Krishnamoorthy, M. Thelakkat and S. Thayumnavan, *J. Phys. Chem. Lett.,* 2010, **1**, 1116; (*c*) J. Xiao, J. Xu, S. Cui, H. Liu, S. Wang and Y, Li, *Org. Lett*., 2008, **10**, 645.

[5] (*a*) L. C. Palilis, H. Murata, M. Uchida and Z. H. Kafafi, *Org. Electron.,* 2003, **4**, 113; (*b*) X. Zhan, A. Haldi, C. Risko, C. K. Chan, W. Zhao, T. V. Timofeeva, A. Korlyukov, M. Y.

Antipin, S. Mongomery, E. Thompson, Z. An, B. Domercq, S. Barlow, A. Kahn, B. Kippelen, J.-L. Bredas, and S. T. Marder, *J. Matter. Chem.,* 2008, **18**, 3157; (*c*) S. A. Ponomarenko and S. Kirchmeyer, *Adv. Polym. Sci.*, 2011, **235**, 33.

[6] (*a*) I. Grabchev and V. Bojinov, *Polym. Degrad. Stabil.,* 2000, **70**, 147; (*b*) T. Z. Philipova and I. Petkov, *J. Appl. Polym. Sci.,* 2001, **80**, 1863.

[7] (*a*) I. Grabchev and R. Betcheva, *J. Photochem. Photobiol. A,* 2001, **142**, 73; (*b*) V. Bojinov and I. Grabchev, *Dyes Pigments.,* 2001, **51**, 57; (*c*) I. Grabchev and T. Konstantinova, *Dyes Pigments.,* 1997, **33**, 197.

[8] Y. Liu, F. Niu, J. Lian, P. Zeng, H. Niu, *Synth. Met.,* 2010, **160**, 2055.

[9] I. Grabchev, C. Petkov and V. Bojinov, *Macromol. Mater. Eng.,* 2002, **287**, 904.

[10] (*a*) A. Iwan and D. Sek, *Prog. Polym. Sci.* 2011, **36**, 1277; (*b*) Z. Ning and H. Tian, *Chem. Commun.* 2009, **45**, 5483; (*c*) Y. Jiang, Y. Wang, J. Hua, J. Tang, B. Li, S. Qian and H. Tian, *Chem. Commun.* 2010, **46**, 4689. (d) W.-Y. Wong and C.-L. Ho, *Coord. Chem. Rev.* 2009, **253**, 1709. (e) W.-Y. Wong and C.-L. Ho, *J. Mater. Chem.* 2009, **19**, 4457. (f) W.-Y. Wong, G.-L. Zhou, X.-M. Yu, H.-S. Kwok, and B.-Z. Tang, *Adv. Funct. Mater.* 2006, **16**, 838. (g) G. Zhou, W.-T. Wong, B. Yao, Z. Xie, and L. Wang, *Angew. Chem. Int. Ed.* 2007, **46**, 1149; (h) X. Xu, X. Yang, J. Dang, G. Zhou, Y. Wu, H. Li and W.-Y. Wong, *Chem. Commun.* 2014, **50**, 2473

[11] W. Jiang, Y. Sun, X. Wang, Q. Wang and W. Xu. *Dyes Pigments,* 2007, **77**, 125.

[12] L. Shi, C. He, D. Zhu, Q. He, Y, Li, Y. Chen, Y. Sun, Y. Fu, D. Wen, H. Cao and J. Cheng. *J. Mater. Chem.* 2012, **22**, 11629.

[13] T. Khanasa, N. Jantasing, S. Morada, N. Leesakul, R. Tarsang, S. Namuangruk, T. Kaewin, S. Jungsuttiwong, T. Sudyoadsuk and V. Promarak, *Eur. J. Org. Chem.,* 2013, **2013**, 2608.

[14] M. Koenemann, J.-H. Hwang, G. Mattern, R. Hoeh and C. Doerr, *US Pat.*, US20110308592A1, 2011.

[15] M. J. Frisch, G. W. Trucks, H. B. Schlegel, G. E. Scuseria, M. A. Robb, J.R. Cheeseman, G. Scalmani, V. Barone, B. Mennucci, G. A. Petersson, H. Nakatsuji, M. Caricato, X. Li, H. P. Hratchian, A. F. Izmaylov, J. Bloino, G. Zheng, J. L. Sonnenberg, M. Hada, M. Ehara, K. Toyota, R. Fukuda, J. Hasegawa, M. Ishida, T. Nakajima, Y. Honda, O. Kitao, H. Nakai, T. Vreven, J. A. Montgomery Jr., J. E. Peralta, F. Ogliaro, M. Bearpark, J. J. Heyd, E. Brothers, K. N. Kudin, V. N. Staroverov, R. Kobayashi, J. Normand, K. Raghavachari, A. Rendell, J. C. Burant, S. S. Iyengar, J. Tomasi, M. Cossi, N. Rega, J. M. Millam, M. Klene, J. E. Knox, J. B. Cross, V. Bakken, C. Adamo, J. Jaramillo, R. Gomperts, R. E. Stratmann, O. Yazyev, A. J. Austin, R. Cammi, C. Pomelli, J. W. Ochterski, R. L. Martin, K. Morokuma, V. G. Zakrzewski, G. A. Voth, P. Salvador, J. J. Dannenberg, S. Dapprich, A. D. Daniels, O. Farkas, J. B. Foresman, J. V. Ortiz, J. Cioslowski, D. J. Fox, Gaussian 09, Revision C.01, Gaussian, Inc., Wallingford CT, 2009.